

A biomimetic collision detection visual neural model coordinating self-and-lateral inhibitions

Jiajun Huang[†], Ziyan Qin, Mengying Wang, Renyuan Liu, and Qinbing Fu^{†,*}

Machine Life and Intelligence Research Centre, School of Mathematics and Information Science, Guangzhou University, China (*qifu@gzhu.edu.cn)

Abstract. Lobula Giant Movement Detectors (LGMD1 and LGMD2), neurons located in the locust's optic lobe, are specialized in detecting approaching objects (looming perception) and have been widely modeled for integration into mobile robots. In bio-inspired robotic implementations of LGMD, inhibitory processes are crucial, as they help maintain selective responses to looming stimuli, enabling reliable collision avoidance. However, current robotic implementations of LGMD models often struggle with nearby translating movements, frequently generating false-positive collision alerts. Recent biological studies have identified trans-medulla afferent (TmA) neurons within the LGMD dendritic region, which may act as a form of self-inhibition (SI). These neurons rapidly suppress intermediate neuronal activities in situ within the LGMD structure, effectively complementing lateral inhibition (LI). Together, SI and LI enhance the specificity of looming responses, reducing interference from translating motions. Despite their biological significance, these mechanisms have yet to be effectively modeled and tested within artificial robotic vision systems. In response, this study introduces a biomimetic visual neural model that incorporates SI and coordinates it with LI during looming perception. The proposed neural computation explicitly activates SI during initial looming events and during translating movements by leveraging spatial correlations within segmented, localized image areas, defined as the local visual field (LVF). This innovative model has been integrated into a bio-inspired micro-robot, named *Colias*, serving as its sole collision detection mechanism. Both offline evaluations and real-world robotic tests demonstrate the efficacy of the biomimetic model in distinguishing looming from translating motions. Consequently, the robot exhibits significantly enhanced collision detection selectivity, closely resembling the capabilities observed in biological organisms.

Keywords: Biomimetic visual model · LGMD · Self-inhibition · Lateral inhibition · Collision detection

1 Introduction

Robust collision detection is essential for safe and efficient navigation in autonomous mobile systems. Biologically inspired visual systems often provide elegant and efficient solutions to collision detection challenges encountered by

intelligent robots. Despite their relatively small brains and limited computational resources, insects possess impressive neural capabilities for detecting and responding to collisions during flight. Locusts, for instance, can navigate vast distances without collisions, even under challenging low-light conditions [1, 2]. Central to this capability are two specialized neurons located in the locust visual system, known as Lobula Giant Movement Detectors (LGMD1 and LGMD2). These neurons exhibit strong sensitivity to objects rapidly approaching on a collision course, while effectively ignoring irrelevant motions, such as lateral translations [3–6]. Thus, the biological principles underlying LGMD neurons and their neural circuitry offer a promising foundation for developing bio-inspired collision detection technologies in robotics.

Inhibitory neural processes are central in shaping the selectivity of loom-sensitive neurons by interacting spatially and temporally with excitatory signals [7–10]. In computational models of these systems, two primary inhibitory mechanisms are commonly simulated. The first, lateral inhibition (LI), enhances spatial resolution and contrast, sharpens the perception of looming object boundaries, and suppresses excessive responses from neighboring neurons [3, 9–12]. The second mechanism, feed-forward inhibition (FFI), reduces neuronal activity when an excessive number of pre-synaptic neurons activate simultaneously, thereby stabilizing the LGMD neuron and preventing over-stimulation [3, 9–11]. These inhibitory processes have been effectively incorporated into neural network models capable of processing visual inputs, whether derived from offline recordings or online sensory streams from robot vision systems [13, 14].

However, current bio-inspired robotic implementations of LGMD models struggle to effectively suppress responses to nearby translating motions, particularly in complex and dynamic visual environments, often resulting in false alarms, as mentioned in a recent review [14]. Recent biological research has uncovered trans-medulla afferent (TmA) neurons within the LGMD’s presynaptic neuropil, functioning likely as a distinct form of inhibition known as self-inhibition (SI) [6]. Unlike other inhibitory mechanisms, SI has been studied explicitly concerning its causal role in shaping neuronal responses. Early investigations into locust visual processing revealed that SI modulates neuronal activity by responding to a neuron’s own excitation, thus enhancing sensitivity to sudden changes or transient visual signals while suppressing background interference [15]. Further research by Rind et al. demonstrated that SI exerts its strongest effects during the initial phase of an object’s approach and when the translating object’s image size remains relatively small [6]. Conversely, LI emerges more gradually, becoming prominent when the image expands significantly near the end of an approaching event [6]. The coordinated interaction between SI and LI thus sharpens neuronal selectivity for looming rather than translating stimuli, highlighting a promising pathway for advancing biomimetic, LGMD-based robotic vision systems.

This study, for the first time, integrated SI and coordinates it with LI in computational models of looming perception. We evaluated the effectiveness of this combined inhibitory mechanism within two neural network models inspired by LGMD1 and LGMD2 neurons [9, 10]. Specifically, SI is implemented by ana-

lyzing spatial correlations within segmented local visual fields (LVF), each corresponding to a specific region of the visual input. The SI mechanism rapidly reduces local excitation when the LVF activation remains below a predefined threshold, operating earlier than LI. Conversely, during genuine looming events, the LVF becomes strongly activated, diminishing SI's influence and allowing LI to dominate the inhibitory interaction, sharpening the neuron's looming-specific response.

To assess the effectiveness and efficiency of the proposed SI mechanism, we conducted both offline evaluations and online robot experiments, comparing our model to original LGMD1 and LGMD2 implementations. The experimental results underscored the efficacy of incorporating and coordinating SI with LI in computational models of looming-sensitive neurons. Although biological studies on SI remain relatively limited, our simulations clearly demonstrated that integrating SI significantly enhances collision selectivity in both LGMD1 and LGMD2 neural models. In practical tests within an experimental arena, the micro-robot exhibited reduced sensitivity to translating movements while maintaining robust and reliable collision detection capabilities.

2 Methods

In this section, the proposed visual neural model will be presented in detail with emphasis laid on how the proposed SI mechanism is incorporated. Specifically, we elaborated on how the SI and LI are coordinated in LGMD1 and LGMD2 models, respectively, as illustrated in Fig. 1. The full description of network processing except the proposed SI algorithm can be found in [9,10]. We present the mathematical equations in discrete forms, which can be programmed directly into robotic systems.

2.1 The proposed SI model in LGMD1-based neural network

The first layer of LGMD1 neural network consists of photoreceptors (P) arranged in a matrix, which capture the luminance of each pixel in an image. The luminance change between successive frames of the image stream is computed and forms the output of this layer [9, 10]. Let $L(x, y, t) \in R^3$ represent the pixel values of the input image, where x, y, and t denote spatial and temporal locations, respectively. The output of this layer is defined as $P(x, y, t) = |L(x, y, t) - L(x, y, t - 1)|$. The output of the P layer forms the input for three separate cell types in the next layer. One type is called excitation cells, computed as $E(x, y, t) = P(x, y, t)$. LI cells, which mimic the functionality of lateral inhibitions, affect their neighboring cells with a certain latency. In the LGMD1 model, the computation of LI is defined as follows:

$$\widehat{E}(x, y, t) = \alpha_1 E(x, y, t) + (1 - \alpha_1) \widehat{E}(x, y, t - 1), \quad \alpha_1 = \Delta t / (\Delta t + \tau_E) \quad (1)$$

$$LI(x, y, t) = \sum_{i=-1}^1 \sum_{j=-1}^1 \widehat{E}(x + i, y + j, t) \cdot W_{LI}(i + 1, j + 1) \quad (2)$$

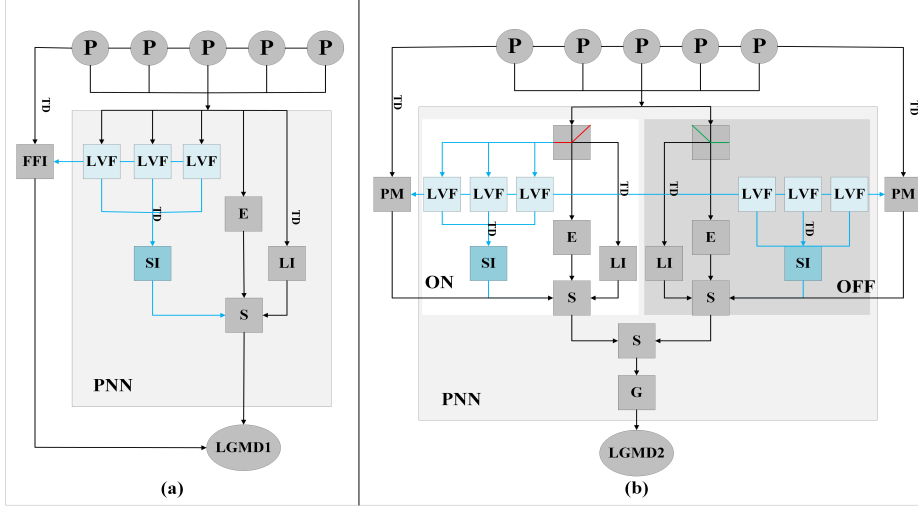


Fig. 1. Schematic of the LGMD1 and LGMD2 neural networks with the proposed SI mechanism. (a) Photoreceptor (P) captures luminance change of the pixels in the field of view, and then transmits the processed information to the partial neural network (PNN) for processing. LGMD1 cell integrates the local excitations processed in the PNN. (b) Visual information is split into ON/OFF parallel pathways with bias in the OFF pathway to realize the specific selectivity of LGMD2. LGMD2 cell integrates the local excitation processed in PNN. The proposed SI mechanism is incorporated into both neural networks through computation in LVF. E: excitation. LI: lateral inhibition. S: summation. LVF: local visual filed. SI: self-inhibition. TD: time delay unit. FFI (or PM): feed-forward inhibition (or photoreceptor mediation). G: grouping.

$W_{LI}(i, j)$ denotes the local convolution matrix that is identical to the original LGMD1 model in [10], which decides the influence by neighboring cells. t_E and Δt are two time constants, where t_E represents the excitation delay, and Δt is the time interval between image frames.

As shown in Fig. 2, SI constitutes the third type of signal formed by the output of P cells. These inputs are based on the average luminance variation received from the LVF each subtending a certain image size. After a shorter latency than LI, the SI can be calculated through the following equations.

$$\hat{P}(x, y, t) = \alpha_2 P(x, y, t) + (1 - \alpha_2) \hat{P}(x, y, t - 1), \quad \alpha_2 = \Delta t / (\Delta t + \tau_P) \quad (3)$$

$$LVF(r, c, t) = \left(\sum_{i=-2}^0 \sum_{j=-2}^0 P(3r + i, 3c + j, t) \right) / 9 \quad (4)$$

$$SI(x, y, t) = \begin{cases} \sum_{i=-1}^1 \sum_{j=-1}^1 \hat{P}(x + i, y + j, t) \cdot W_{SI}(i, j), & \text{if } LVF(r, c, t) \leq \gamma_1, \\ \beta_1 \sum_{i=-1}^1 \sum_{j=-1}^1 \hat{P}(x + i, y + j, t) \cdot W_{SI}(i, j), & \text{otherwise} \end{cases} \quad (5)$$

τ_P represents the photoreceptor delay, while $LVF(r, c, t)$ denotes the average luminance variation at the position $(r, c) = \left\lceil \frac{(x, y)}{3} \right\rceil$. γ_1 denotes a small real number

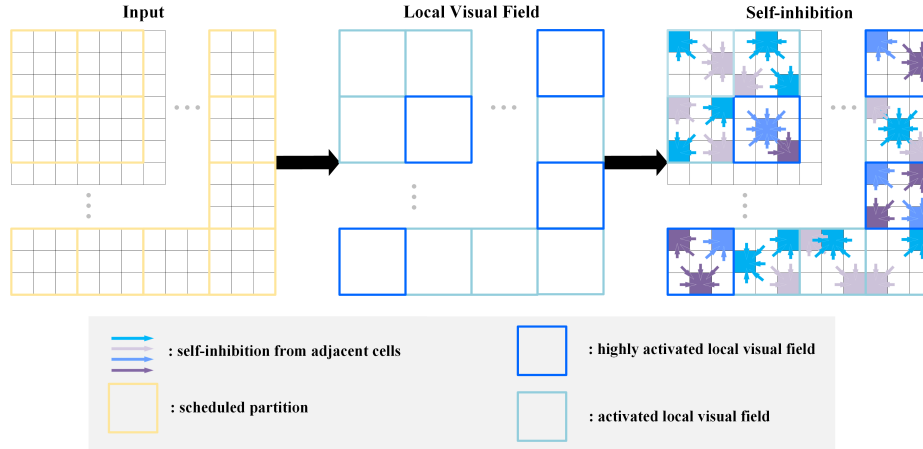


Fig. 2. The proposed SI mechanism operates by leveraging spatially distributed local visual fields (LVFs), with the strength of SI computed through spatial convolution across these fields. Each LVF comprises nine local SI units, where the activation level of each unit is determined by the average neuronal activity within its respective LVF.

as a threshold gate, and β_1 is a suppressive coefficient. W_{SI} represents the convolution kernel that satisfies

$$W_{SI} = \begin{bmatrix} \frac{1}{8} & \frac{1}{4} & \frac{1}{8} \\ \frac{1}{4} & 1 & \frac{1}{4} \\ \frac{1}{8} & \frac{1}{4} & \frac{1}{8} \end{bmatrix} \quad (6)$$

Subsequently, as shown in Fig. 1, the LI, SI, and E are summed together in S layer as

$$S(x, y, t) = E(x, y, t) - \theta_1 \cdot SI(x, y, t) - \theta_2 \cdot LI(x, y, t) \quad (7)$$

θ_1 and θ_2 are the coefficients with SI and LI, respectively. Finally, LGMD1 unit integrates remaining excitation to form the membrane potential, normalized into $[0.5, 1]$ as

$$k(t) = \sum_{x=1}^M \sum_{y=1}^N S(x, y, t), \quad K(t) = 1 / (1 + e^{-\frac{k(t)}{\alpha_3 MN}}) \quad (8)$$

2.2 The proposed SI model in LGMD2-based neural network

We move on introducing how the proposed SI mechanism is integrated into the LGMD2 neural network model. The main difference between LGMD1 and LGMD2 is the signal bifurcation of photoreceptors into ON/OFF channels through operations of half-wave rectification. The entire process can be defined as

$$P(x, y, t) = L(x, y, t) - L(x, y, t - 1) \quad (9)$$

$$P_{on}(x, y, t) = [P(x, y, t)]^+ + \alpha_4 P_{on}(x, y, t - 1) \quad (10)$$

$$P_{off}(x, y, t) = -[P(x, y, t)]^- + \alpha_4 P_{off}(x, y, t - 1) \quad (11)$$

Table 1. Parameters of the proposed method

| Parameter | Description | Value |
|--------------------------------|--|------------------|
| τ_E | latency with LI-flow | $6 \sim 10$ (ms) |
| τ_P | latency with SI-flow | $3 \sim 5$ (ms) |
| β_1, β_2 | local biases in SI piecewise functions | $0.01 \sim 0.5$ |
| γ_1 | activation threshold of LVF | $0.005 \sim 3$ |
| $\theta_1, \theta_3, \theta_4$ | coefficients with SI calculating S | $2 \sim 5$ |
| M, N | row, column of input image streams | adaptable |

$[x]^+$ and $[x]^-$ denote $\max(0, x)$ and $\min(x, 0)$, respectively.

The subsequent E, I, and S layers are accordingly divided into ON/OFF channels considering visual contrast change as shown in Fig. 1. The whole process can be referred in the comparative model [9], which is omitted. The emphasis herein is laid on incorporating the proposed SI mechanism to be coordinated with LI. Considering visual contrast separated by ON/OFF channels, the LVF is incorporated in each pathway. Taking the neural computation of ON channels as examples, the SI is computed through

$$\hat{P}_{on}(x, y, t) = \alpha_{on} P_{on}(x, y, t) + (1 - \alpha_{on}) \hat{P}_{on}(x, y, t - 1) \quad (12)$$

$$LVF_{on}(r, c, t) = \left(\sum_{i=-2}^0 \sum_{j=-2}^0 \hat{P}_{on}(3r + i, 3c + j, t) \right) / 9 \quad (13)$$

$$SI_{on}(x, y, t) = \begin{cases} \sum_{i=-1}^1 \sum_{j=-1}^1 \hat{P}_{on}(x + i, y + j, t) \cdot W_{on}(i, j), & \text{if } LVF_{on}(r, c, t) \leq \gamma_1, \\ \beta_2 \sum_{i=-1}^1 \sum_{j=-1}^1 \hat{P}_{on}(x + i, y + j, t) \cdot W_{on}(i, j), & \text{otherwise} \end{cases} \quad (14)$$

$$W_{on} = \begin{bmatrix} \frac{1}{2} & 1 & \frac{1}{2} \\ 1 & 4 & 1 \\ \frac{1}{2} & 1 & \frac{1}{2} \end{bmatrix} \quad (15)$$

The computations of SI in OFF channels conforms to those in ON channels. The inhibitory bias is put forth in ON channels to suppress ON-contrast to achieve the LGMD2's specific selectivity to OFF-contrast motions. Thus, the convolution matrix in OFF channels is halved by W_{on} .

After generating local ON/OFF excitation and inhibition, there are ON/OFF-S units in both channels, that is,

$$S_{on}(x, y, t) = [E_{on}(x, y, t) - \theta_3 * SI_{on}(x, y, t) - w_1(t) * LI_{on}(x, y, t)]^+ \quad (16)$$

$$S_{off}(x, y, t) = [E_{off}(x, y, t) - \theta_4 * SI_{off}(x, y, t) - w_2(t) * LI_{off}(x, y, t)]^+ \quad (17)$$

θ_3 and θ_4 are coefficients in the ON and OFF pathways, respectively. $w_1(t)$ and $w_2(t)$ are time-varying coefficients calculated by the adaptive inhibition mechanism presented in [9]. The remaining neural computation in LGMD2 network also conforms to [9].

The parameter configurations employed in this study are summarized in Table 1, while remaining parameters are consistent with those from the original

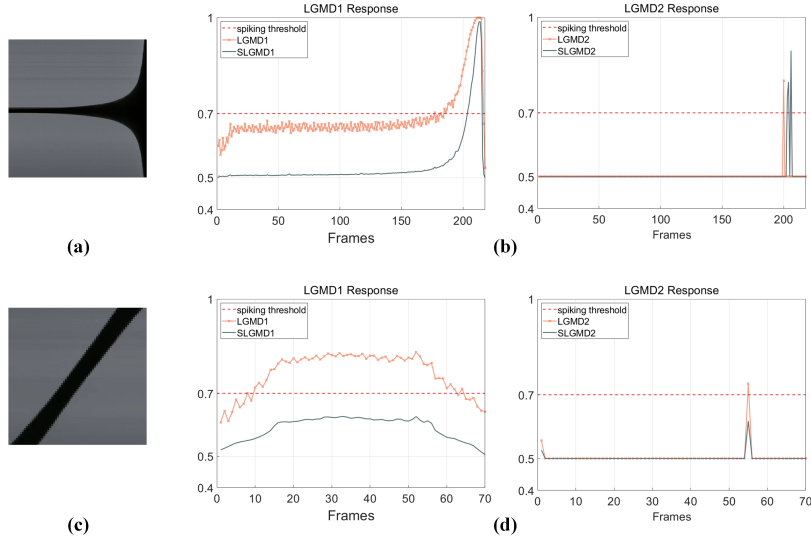


Fig. 3. Results of comparative models challenged by a dark ball approaching and translating within a bright background in a real physical scene. (a) Looming stimulus shows the increase of image size (dark pixels) during approaching over time. (b) Outputs of LGMD1 and SLGMD1 (LGMD1 with SI mechanism), LGMD2 and SLGMD2 (LGMD2 with SI mechanism) in response to the looming stimulus. (c) Translating stimulus shows the change of ball position over time and the image size (dark pixels) retains almost consistent. (d) Response to the translating stimulus. The horizontal dashed line indicates a predefined spiking threshold to compare with membrane potentials.

LGMD1 and LGMD2 models [9, 10]. All parameter values were selected to optimize the functional performance of the proposed biologically plausible mechanisms, particularly to emulate the SI characteristics. Notably, the convolution matrices differ between LI and SI. Specifically, the center element is set to zero for LI, reflecting a spatially distributed inhibition signal, whereas it is non-zero for SI, enabling direct local suppression of neuronal excitation.

Currently, due to the relatively small parameter set involved, there is no established learning approach for parameter selection. In offline experiments, input resolution of 480×720 pixels was used. In online robotic experiments, the mounted camera captures images at a resolution of 99×72 pixels, with the sampling frequency regulated at around 30 Hz.

3 Experimental Results and Analysis

Within this section, our experiments will be described to illustrate how the coordination of SI and LI work to suppress translating motion in order to enhance the selectivity in neural networks for collision detection. All the experiments can be divided into two categories of offline and online tests. In the former category, the input stimuli are divided into two types, one is a rolling ball movement in a simple context and another is outdoor shooting scene. We compared the response

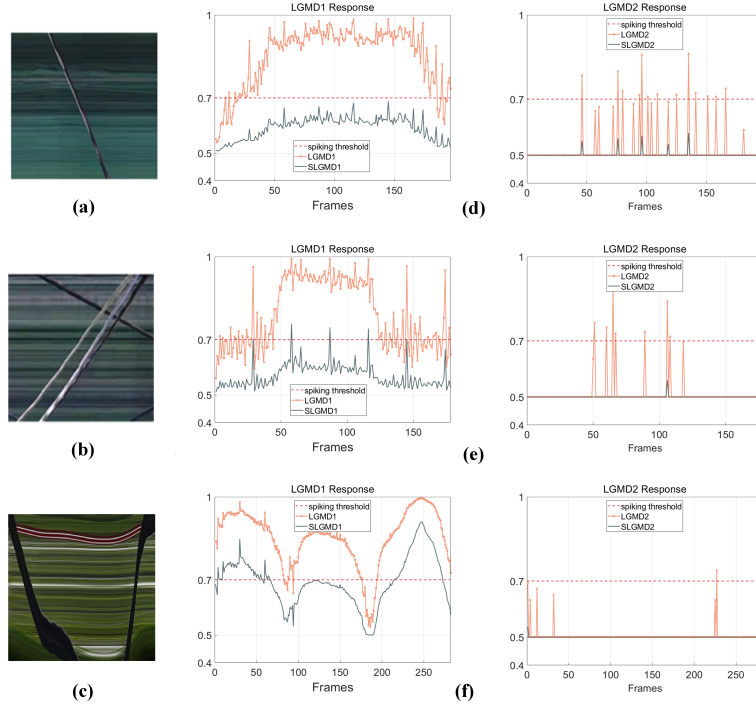


Fig. 4. Results of comparative models challenged by natural motion stimuli. (a) Translating stimulus of a pedestrian passing by against dynamic natural background. (b) Translating stimulus of a ground of people passing by. (c) Translating stimulus recorded by an aerial robot shifting with the image size (dark pixels) changing over time. (d),(e),(f) Outputs of LGMD1 and SLGMD1 (LGMD1 with SI mechanism), LGMD2 and SLGMD2 (LGMD2 with SI mechanism) in response to each translating stimulus.

and selectivity of the model with the original LGMD1 [10] and LGMD2 [9] models without the proposed method.

3.1 Method evaluations

Firstly, the stimulus consists primarily of various motion patterns of a rolling ball recorded in indoor laboratory settings. Compared to previous synthetic stimuli, this setup introduces more background noise, and the rolling ball's speed is not constant. In these tests, the proposed method was evaluated using a darker object moving in depth against a bright background, incorporating both looming and translating movements. As shown in Fig. 3, the LGMD with SI (SLGMD) models effectively suppressed translating motion while maintaining a selective response to approaching objects. Furthermore, the responses of SLGMD models were noticeably smoother than those of the original models, suggesting that the incorporation of SI could help reduce real-world noise (see Figures 3b and 3d).

Secondly, under outdoor translating stimulation, the comparative models were tested using real-world visual stimuli recorded by camera. Compared to

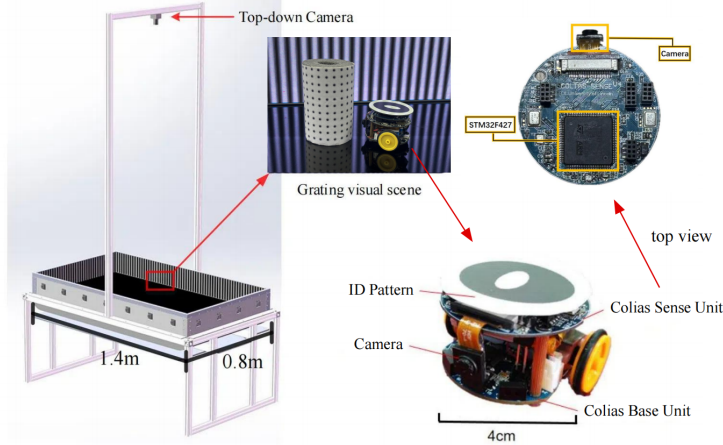


Fig. 5. Illustration of the experimental arena and the *Colias* micro-robot [16].

the structured indoor scenes, the outdoor environment introduced more complex and dynamic backgrounds, making it more challenging for the model to recognize object motion patterns. As shown in Fig. 4, both SLGMD1 and SLGMD2 models demonstrated a notable suppression of translating motions in these complex settings compared to the original models. Additionally, Fig. 4 reveals that the SLGMD2 model exhibited the best performance upon depressing translating motions.

3.2 Robot online tests

This part presents the performance of the proposed biomimetic visual system as embedded vision in *Colias* micro-robot [16]. The experiments were structured sequentially with two primary objectives. Initially, the focus was on evaluating the effectiveness of the combined SI and LI mechanisms in robotic systems for suppressing translational motion (i.e., open-loop tests). Subsequently, the emphasis shifted toward assessing the robustness of fundamental collision detection during autonomous robot navigation (i.e., closed-loop tests). Consequently, a direct comparison of collision detection success rates with the original models was not performed in this paper. The experimental settings of robot tests and arena are collectively illustrated in Fig. 5.

Under open-loop tests, we employed a translating robot motion to test both the proposed method and the original models. During these open-loop tests, the motion unit of the stimulated robot was deactivated, and its responses to the visual stimuli were collected and visualized (as shown in Fig. 6). These experiments aimed to verify whether the coordination of SI and LI effectively suppresses translating motion patterns, thereby enhancing selectivity of such biomimetic system for looming objects.

Fig. 6 presents the statistical outputs of each model under repeated translating motion patterns. Both LGMD1 and LGMD2 original models exhibited strong

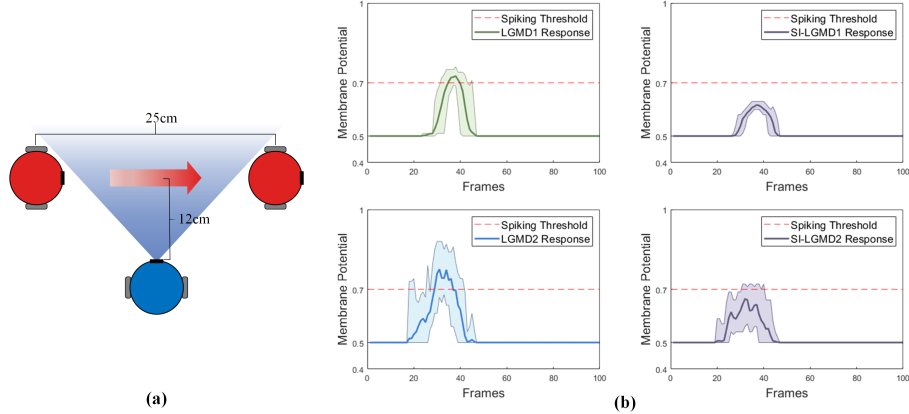


Fig. 6. Statistical results of robot challenged through repeated open-loop translating stimuli. (a) The experimental setup involves a robot translating at a specific distance from the stimulated robot where the models are implemented. (b) Responses of comparative models including mean and variance of membrane potentials. The horizontal dashed line indicates a predefined spiking threshold for collision detection.

responses to translational movements. While LGMD1 responded more strongly than LGMD2, both models frequently misidentified translational stimuli as potential collisions, resulting in false alarms (membrane potential exceeding the spiking threshold). In contrast, the SI-LI models (SLGMD1 and SLGMD2) effectively suppressed responses to translational movements by dynamically adjusting inhibition intensity within the LVF, aligning with results of previous offline evaluations.

In arena tests, we conducted autonomous navigation with the results illustrated in Fig. 7. The robot configuration aligned with the comparative study [9]. The results highlighted the efficacy of coordinating SI and LI in robotic embedded vision for real-time collision detection and avoidance in dynamic environments encompassed by grating-patterned stimulation. Previous experiments demonstrated that the proposed method significantly depresses translating stimuli. In the arena tests, the robot maintained strong collision selectivity, navigating autonomously without human intervention and avoiding collisions within the arena for an extended period. These findings also confirmed that the modeling of SI can be generalized to neural network-based robotic vision systems for collision perception.

4 Discussions

The systematic experiments conducted in this study demonstrated that the proposed biomimetic visual neural model works effectively to suppress translating motion by coordinating SI and LI mechanisms, thereby enhancing the selectivity of LGMD models for looming objects. Robot online experiments verified the effectiveness of SI mechanism integrated into embedded vision to reduce responsive action of robot to translating stimuli while maintaining the robustness

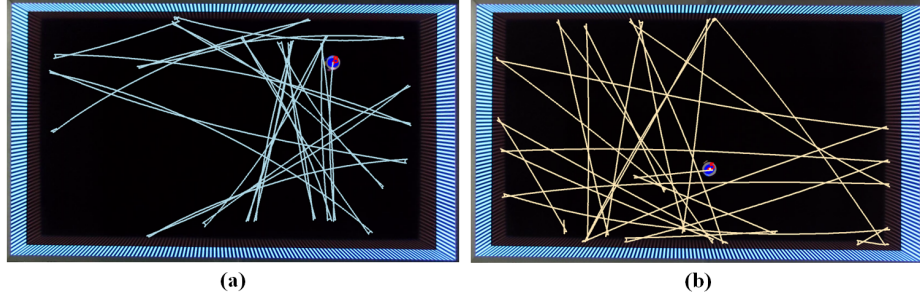


Fig. 7. Robot arena tests results of investigating collision detection capabilities: (a) The LGMD1 model with the proposed SI mechanism is integrated into the embedded visual module of *Colias*. The trajectories of robot over a 5-minute navigation are recorded and depicted. The robot runs autonomously at around 4 cm/s, and turns randomly to left or right when detecting potential collision. The arena walls display sine-grating shifting pattern. (b) The case of LGMD2 model with the proposed SI mechanism under same settings.

in collision detection during autonomous navigation. Additionally, the experimental results confirmed the generalization ability of the proposed SI algorithm in neural networks for collision perception, as it worked effectively for either LGMD1/LGMD2 models.

This modeling research also presents several interesting findings. First, Rind, et al. identified key differences between SI and LI: (1) SI takes effect earlier than LI, and (2) SI is most effective when changes over visual field are minimal, while LI dominates when luminance varies significantly [6]. To implement these features, this study incorporates different delay parameters associated with SI/LI, and utilizes down-sampled LVF to indicate local image size over time. Second, Rind's research on SI-LI interaction found that while SI alone does not suppress responses to looming, the coexistence of SI and LI enhances inhibition of looming responses and effectively suppresses translating motion, maintaining selectivity for looming objects [6]. This phenomenon was reproduced in the biomimetic system demonstrated by our *Colias* robot, which validated the biological relevance of the proposed method. At last, tests under realistic stimulus conditions showed that the incorporation of SI resulted in smoother response outputs compared to the original model, suggesting a potential noise reduction capability of the proposed method.

Acknowledgment

This research was supported by the National Natural Science Foundation of China under Grant No. 62376063. Qinbing Fu and Jiajun Huang share first authorship. Corresponding author: Qinbing Fu (qifu@gzhu.edu.cn).

References

1. E. Warrant and M. Dacke, "Visual navigation in nocturnal insects," *Physiology*, vol. 31, no. 3, pp. 182–192, 2016.
2. E. Baird, E. Kreiss, W. Wcislo, E. Warrant, and M. Dacke, "Nocturnal insects use optic flow for flight control," *Biology Letters*, vol. 7, no. 4, pp. 499–501, 2011.
3. F. C. Rind and D. Bramwell, "Neural network based on the input organization of an identified neuron signaling impending collision," *Journal of Neurophysiology*, vol. 75, no. 3, pp. 967–985, 1996.
4. M. O'shea and C. F. Rowell, "The neuronal basis of a sensory analyser, the acridid movement detector system. ii. response decrement, convergence, and the nature of the excitatory afferents to the fan-like dendrites of the lgmd," *Journal of Experimental Biology*, vol. 65, no. 2, pp. 289–308, 1976.
5. P. J. Simmons and F. C. Rind, "Responses to object approach by a wide field visual neurone, the lgmd2 of the locust: characterization and image cues," *Journal of Comparative Physiology A*, vol. 180, pp. 203–214, 1997.
6. F. C. Rind, S. Wernitznig, P. Pölt, A. Zankel, D. Gütl, J. Sztarker, and G. Leitinger, "Two identified looming detectors in the locust: ubiquitous lateral connections among their inputs contribute to selective responses to looming objects," *Scientific Reports*, vol. 6, no. 1, p. 35525, 2016.
7. S. Bermúdez i Badia, U. Bernardet, and P. F. Verschure, "Non-linear neuronal responses as an emergent property of afferent networks: A case study of the locust lobula giant movement detector," *PLoS Computational Biology*, vol. 6, no. 3, p. e1000701, 2010.
8. Q. Fu, C. Hu, J. Peng, and S. Yue, "Shaping the collision selectivity in a looming sensitive neuron model with parallel on and off pathways and spike frequency adaptation," *Neural Networks*, vol. 106, pp. 127–143, 2018.
9. Q. Fu, C. Hu, J. Peng, F. C. Rind, and S. Yue, "A robust collision perception visual neural network with specific selectivity to darker objects," *IEEE Transactions on Cybernetics*, vol. 50, no. 12, pp. 5074–5088, 2019.
10. S. Yue and F. C. Rind, "Collision detection in complex dynamic scenes using an LGMD-based visual neural network with feature enhancement," *IEEE Transactions on Neural Networks*, vol. 17, no. 3, pp. 705–716, 2006.
11. E. G. Olson, T. K. Wiens, and J. R. Gray, "A model of feedforward, global, and lateral inhibition in the locust visual system predicts responses to looming stimuli," *Biological Cybernetics*, vol. 115, no. 3, pp. 245–265, 2021.
12. F. Lei, Z. Peng, M. Liu, J. Peng, V. Cuturidis, and S. Yue, "A robust visual system for looming cue detection against translating motion," *IEEE Transactions on Neural Networks and Learning Systems*, vol. 34, no. 11, pp. 8362–8376, 2022.
13. Q. Fu, H. Wang, C. Hu, and S. Yue, "Towards computational models and applications of insect visual systems for motion perception: A review," *Artificial Life*, vol. 25, no. 3, pp. 263–311, 2019.
14. Q. Fu, "Motion perception based on on/off channels: a survey," *Neural Networks*, vol. 165, pp. 1–18, 2023.
15. D. Osorio, "Mechanisms of early visual processing in the medulla of the locust optic lobe: how self-inhibition, spatial-pooling, and signal rectification contribute to the properties of transient cells," *Visual Neuroscience*, vol. 7, no. 4, pp. 345–355, 1991.
16. C. Hu, Q. Fu, and S. Yue, "Colias IV: The affordable micro robot platform with bio-inspired vision," in *Annual Conference Towards Autonomous Robotic Systems*. Springer, 2018, pp. 197–208.